Structural and Impact Loads for the Flexible Airplane During Water Landings

EDWARD WIDMAYER, JR.* AND ROBERT H. SCHWAB*

The Martin Company

Summary

A method for calculating structural loads due to water landing impact has been developed. The results of this method have, for the most part, been substantiated by the results of an experimental program in which both the hull bottom loads and the acceleration response of the M-270 airplane were measured. Past research has shown that the impact loads are dependent on rate-of-descent, trim angle, landing speed, hull shape, and degree of flexibility of the entire airplane. The method presented herein includes the above factors and emphasizes the dependency of the hydrodynamic loads on the flexible airplane response. Calculations are made for both a rigid and a flexible airplane and are compared with the experimental results. In using modern computing methods it was found that continuous trim variations and load input at several stations were possible.

Symbols

A	=	acceleration
a_n	=	coefficient of nth vibratory mode
b_x	=	distance in x direction from mass center of airplane to mass station, positive aft
C	=	wetted width of hull
C_p	=	pressure coefficient
D	=	viscous damping coefficient
e	=	base of Naperion logarithm
F_s	=	hydrodynamic force acting through step of airplane normal to keel, positive down
G	=	structural damping coefficient
g	=	acceleration due to gravity
Z_1	=	draft of hull after chine immersion
Z_c	=	draft of hull at chine immersion
l_k	=	wetted length of hull measured from step
m	=	mass considered to act at a given airplane station
M_s	=	hydrodynamic moment about step, positive nose up
M_w	=	virtual mass of water
P_{ave}, P_{max}	=	hydrodynamic pressures
t	=	time
V_h	=	forward speed
V_n	=	speed normal to keel
x	=	coordinate in fore and aft direction of airplane
y	=	coordinate in span direction
z	=	coordinate in direction normal to keel
Δ	=	hydrodynamic force associated with dynamic pressure, positive down
μ	=	Wagner's function for spray thickness
ρ	=	density of water
φ	=	slope of deformed structure
ω_n	=	circular frequency of nth mode
τ	=	trim angle, positive nose up

Superscripts and Subscripts

$(\ddot{\ })$, $(\dot{\ })$	=	time derivations
c	=	at chine or chine immersion
ave	=	average
max	=	maximum
s	=	at step
0	=	initial condition
n, r, s	=	modal designation
n	=	normal
h	=	horizontal

Presented at the Aeroelasticity—II Session, Twenty-Fifth Annual Meeting, IAS, New York, January 28–31, 1957.

* Group Engineer, Dynamics Section.

Introduction

THE SUBJECT MATTER of this paper forms a small portion of the results of a research program initiated by the Bureau of Aeronautics to study loads developed during impact of water landings. (See references 1 and 2.) It is felt that the results of this work represent a significant advance in the treatment of the landing impact problem and form a base from which analytical treatment may be extended to cover landings in any type of sea. Historically, the water landing impact problem has been separated into two distinct parts: the determination of the maximum water loads, and the determination of the transient structural loads arising from the structural response to these water loads.[3] This separation of the generation of water loads from the structural response has been long recognized as an artificial device, and a method of including the influence of wing structural flexibility on the water loads has been given in reference 4.

For relatively rigid seaplanes, the transient structural loads determined from the maximum water loads generally have been sufficient for engineering purposes. However, for more flexible seaplanes a formulation of the impact problem that allows the full interaction of the hydrodynamic forces and the dynamic response of the elastic seaplane is desired. Since the dynamic response of an elastic seaplane is a function of rate-of-load application as well as the peak value of the load, the formulation of the impact problem should permit rapid solution for a wide parametric variation of initial landing conditions.

An analytical method of treating the step landing impact problem in smooth water is developed. It gives in "closed" form the simultaneous determination of both the water loads and the transient structural loads. In solving the resulting equations of motion, a procedure using an electronic analog computer has been developed which permits the rapid solution of the landing problem for a large range of initial landing conditions. Solutions of the impact problem obtained for the M-270 seaplane, considered as being completely rigid and as being completely flexible, for a

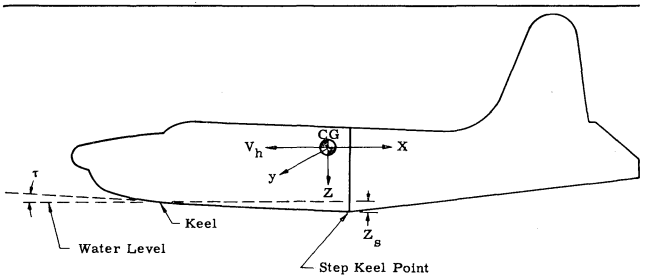

FIG. 1. Airplane coordinate system.

range of landing conditions are presented and discussed.

The experimental program for the M-270 airplane is briefly discussed. While this program includes extensive experimental measurements of hull bottom pressures, loads, and structural response, only those results directly applicable to this paper are presented. These experimental results are compared with the results of the theoretical analysis. These comparisons are discussed with respect to both the time variation and the maximum values of the various parameters.

THEORETICAL LANDING LOADS ANALYSIS

The airplane coordinate system is shown in Fig. 1. The displacement of any point in the elastic structure is considered to be represented by the sum of the displacements of that point in each mode of vibration including the zero frequency modes. This may be expressed as follows:

$$Z(x, y) = b(x) + a_n Z_n(x, y) \tag{1}$$

The selection of the modal shapes necessary to approximate the structure during impact accurately is governed largely by the vibratory characteristics of the structure and by the time variation of the applied forces. Bases for the inclusion of a sufficient number of modes have been discussed in previous literature on dynamic response and, therefore, will not be discussed here. For the purpose of this paper the displacement of an airplane element in the elastic case is represented by the contributions of the first four flexural airplane modes in conjunction with rigid body translation and rotation. The displacement of an airplane element in the rigid body case is represented by rigid body translation and rotation.

The hydrodynamic forces and moments generated during a step landing are given by Eqs. (2) and (3).

$$F_s = -\Delta - M_w(\ddot{Z}_s - 0.65 l_k \ddot{\tau}) \tag{2}$$

$$M_s = -F_s(0.65 l_k) \tag{3}$$

The theoretical development of Eqs. (2) and (3) is discussed in detail in references 1 and 2 and will not be treated here. However, the results of the theory necessary for a solution to the equations of motion are discussed below.

The term Δ is associated with effects of the dynamic pressure and is given in Eq. (4).

$$\Delta = \rho V_n |V_n| \int_0^{l_k} C_p C(dl_k) \tag{4}$$

where

$$V_n = \dot{Z}_s + V_h \sin \tau - 0.65 l_k \dot{\tau}$$

In this expression the influence of the vertical velocity of the wetted surface is obtained from contributions of $\dot{Z}$ and $\dot{\tau}$. The distance $0.65 l_k$ is assumed to be the location of the center of pressure of the wetted surface from the step of the keel. The effect of planning forces is reflected in the contributions of $V_h \sin \tau$.

The functions C_p and C have discontinuities at the point of chine immersion. The wetted width, C, varies with draft until the chines are immersed, and for further increase in draft, C is assumed to be constant. Prior to chine immersion, C_p is given by the following equation:

$$C_p = \frac{P_{ave}}{P_{max}} \frac{1}{\sin^2 \tau + \mu^2 \cos^2 \tau + (Z_c/C)^2 \sin^2 \tau}$$

After chine immersion, C_p is given by

$$C_p = \frac{P_{ave}}{P_{max}} \frac{1}{\sin^2 \tau [1 + (Z_c/C)^2 + (Z_1/C)]^2}$$

In these expressions for C_p the quantity P_{ave}/P_{max} is a function of the draft. Knowing the variation C_p, C, and l_k as a function of Z_s for a given value of τ, the integral $\int_0^{l_k} C_p C(dl_k)$ could be evaluated.

The second term in Eq. (2) is associated with the forces given by

$$M_w = \rho \int_0^{l_k} C^2 dl_k$$

These are the well-known "apparent mass" effects. With the variation of C with Z_s known, $\int_0^{l_k} C^2 dl_k$ may be evaluated for a given τ.

The moment about the step is taken as that due to the water force acting through the center of pressure.

The hydrodynamic forces acting on a section of the hull are complicated by variations in trim, complex form factors, chine-immersions effects, and three-dimensional flow. The treatment of these parameters may be made by any rationally acceptable methods of analysis (cf. reference 2 or 5). It is important that rational expressions for force and moment in terms of the parameters of the dynamic problem be available.

In the actual evaluation of the above integrals, it was convenient to utilize digital machine computational methods. The integrals were evaluated for τ equal to 3°, 6°, and 9° for the range of Z_s expected to be encountered by the airplane, and the results were shown in graphical form. It was then found to be possible to approximate the curves for constant τ with analytic expressions in which Z_s and τ appeared as simple functions. Further, it was found that the family of curves was adequately given when the value

of τ was permitted to vary. Consequently, when the simple analytic expressions for the integrals are substituted into the equation for the hydrodynamic force, the restriction of the landing conditions to constant values of trim is no longer necessary to the solution of the landing impact problem.

The expressions for the $\int_0^{l_k} C_p C dl_k$ and $\int_0^{l_k} C^2 dl_k$ were found to be as follows for the M-270 airplane:

$$\left.\begin{aligned} 0 < Z_s < 0.2Z_c \qquad & \int_0^{l_k} C_p C dl_k = \frac{4.59 - 12.0\tau}{\tau} Z \\ 0.2 < Z_s < Z_c \qquad & \int_0^{l_k} C_p C dl_k = \frac{1.31 - 2.2\tau}{\tau} (e^{2Z} - 0.82) \\ Z_c < Z \qquad & \int_0^{l_k} C_p C dl_k = \frac{-87.1 + 94.5e^{-3.3(Z-1)} + 40.1 - 34.2e^{-1.88(Z-1)}}{\tau} \end{aligned}\right\} \tag{5}$$

and

$$\left.\begin{aligned} 0 < Z_s < Z_c \qquad & \pi\rho \int_0^{l_k} C^2 dl_k = (17.8/\tau) Z (Z^2 + 0.1435) \\ Z_c < Z \qquad & \pi\rho \int_0^{l_k} C^2 dl_k = (76.8/\tau) (Z - 0.735) \end{aligned}\right\} \tag{5a}$$

In the present problem, these expressions gave excellent approximations of the integrals for values of Z_s up to 36 in. and gave reasonable agreement for values of Z_s in excess of 36 in. It should be noted that for that portion of the landing most important to the airplane response—i.e., during the build-up to maximum force—these analytical expressions are most valid.

The forces arising from the explicit variation of trim in Eq. (2) include a component due to the dynamic pressure and a component due to the virtual mass. In the force due to dynamic pressure, V_n has components of velocity arising from both the trim and the rate of pitch of the airplane. During the early portions of impact the contribution due to the instantaneous trim does not vary appreciably. However, the contribution due to the rate of change in trim, $\dot{\tau}$, in those cases where there is large wetted length, may become important. The component of force due to the acceleration of the "virtual" mass of water is affected by the angular acceleration. In those cases where the wetted length is long and the pitching acceleration is large, the effect of this acceleration on the forces is appreciable.

In permitting trim variation, it was necessary to determine the centroid of the pressure distribution acting on the bottom. For the high-beam loaded hull where chine immersion occurs early in impact, the center of pressure is taken at 65 per cent of the instantaneous value of the wetted length. The factors on which the selection of $0.65l_k$ is based are discussed in reference 2. The location of the pressure centroid is of importance for landings at low initial values of trim where the wetted length may be expected to exceed four times the beam of the hull.

Equations of Motion

The equations of motion relating the behavior of the airplane to the hydrodynamic forces encountered during impact may be derived with any of usual procedures of this type of analysis. The following equations are obtained:

$$\left.\begin{aligned} -\ddot{Z}_0 + (F_s/\textstyle\sum m) &= 0 \\ & \qquad n = 1, 2, 3, 4 \\ -\ddot{\tau} + \frac{F_s b_s + M_s}{\sum m b^2_{(x)}} &= 0 \\ -\ddot{Z}_n - g\omega_n \dot{Z}_n - \omega_n{}^2 Z_n + \frac{(a_n)_s F_s + \phi_s M_s}{\sum (a_n)^2 m} &= 0 \end{aligned}\right\} \tag{6}$$

when the initial values of $\dot{Z}_s$, τ, and V_n are given, Eqs. (6) may then be solved for the $Z_s(t)$, $\tau(t)$, $F_s(t)$, and $M_s(t)$. In addition, the acceleration at any mass station may be obtained by the use of the following relation:

$$\ddot{Z}_{(x\,y)} = a_0 \ddot{Z}_0 + b_{(x)}\, \ddot{\tau} + \sum_1^n a(x_1 y)_n \ddot{Z}_n$$

With these quantities known, the impact forces and structural response are determined, and the distribution of load over the structure may be studied.

From an examination of Eqs. (6), it can be seen that the equations are nonlinear functions of Z, $\dot{Z}$, $\ddot{Z}$, and τ. Previously, when it was sufficient to treat the landing problem as the rigid body, the translatory response to the hydrodynamic forcing function solutions was obtained either by a step-by-step integration or by use of an analog computer. The inclusion of additional degrees of freedom has increased the complexity of the problem and has made the analog solution attractive.

The solution to Eqs. (6) has been obtained readily by using an electronic analog computer. The left-hand side of Eqs. (6), giving the forces arising within the structure, presents no difficulty in machine programing. The use of a simple analytical expression for the hydrodynamic force and moments, while requiring additional machines, may also be readily programed. Continuous records of hydrodynamic forces and mo-

ments, displacement and structural accelerations, shears, and bending moments may then be obtained.

Experimental Program

A test program was initiated to obtain experimental data for correlation with theoretical hull bottom water loads and airplane accelerations during landing impact of the M-270 airplane.

Instrumentation for the tests consisted of a total of 49 transducers, which included 13 accelerometers, 20 flush-type pressure transducers, and 16 strain gages. The distribution of transducers in the airplane is shown in Fig. 2. The output of the transducers was recorded on oscillographs.

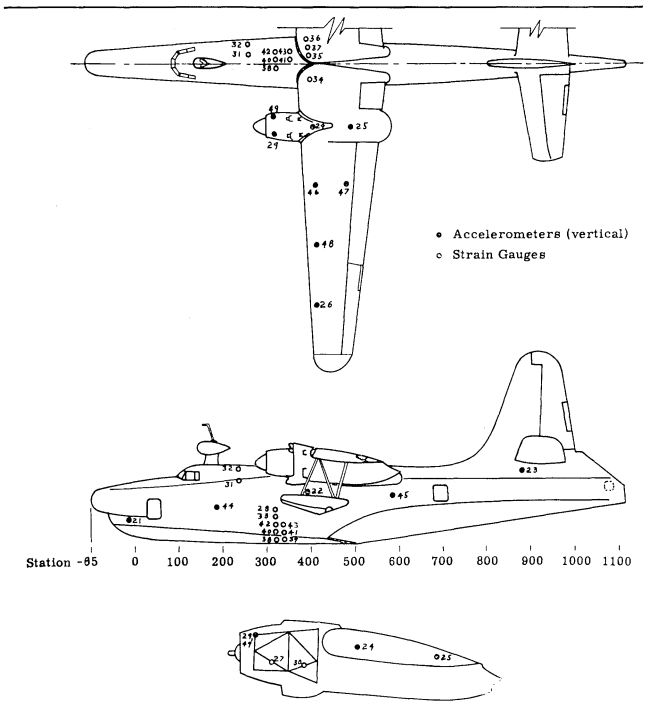

Fig. 2. Location of instrumentation on aircraft structure.

Cable No.	Item	Location
21	accelerometer	hull sta. 18, w.l. 49½, ℄ of ship
22	accelerometer	hull sta. 396, w.l. 130, ℄ of ship
23	accelerometer	hull sta. 885, w.l. 160, ℄ of ship
24	accelerometer	l. wing sta. 147.5, front spar
25	accelerometer	l. wing sta. 147.5, rear spar
26	accelerometer	l. wing sta. 600, front spar
27	strain gage	engine mount tube, center of tube
28	strain gage	vertical shear, hull sta. 328, web of floor frame
29	accelerometer	engine mount, l.h. forward
30	strain gage	engine mount tube, center of tube
31	strain gage	sta. 236, center of longeron, r.h. side
32	strain gage	sta. 236, walkway stringer, r.h. side
33	strain gage	hull sta. 328, ℄ top chord floor frame
34	strain gage	hull sta. 386, center of longeron, l.h. side
35	strain gage	hull sta. 386, walkway stringer, r.h. side
36	strain gage	hull sta. 386, outboard face of longeron, r.h. side
37	strain gage	hull sta. 386, inboard face of longeron, r.h. side
38	strain gage	top of keel former, sta. 321
39	strain gage	hull bottom midway between S-0 and S-1, sta. 338½
40	strain gage	top of S-0 at ℄ of vertical stiffener to stringer attached at sta. 328
41	strain gage	top of S-0 at ℄ of vertical stiffener between sta. 328 and 350
42	strain gage	top of S-2 at ℄ of vertical stiffener at sta. 328
43	strain gage	top of S-2 at ℄ of vertical stiffener between sta. 328 and 350
44	accelerometer	℄ hull, sta. 180
45	accelerometer	℄ hull, sta. 574
46	accelerometer	l. wing, sta. 300, front spar
47	accelerometer	l. wing, sta. 300, rear spar
48	accelerometer	l. wing, sta. 450, front spar
49	accelerometer	engine mount, l.h. forward

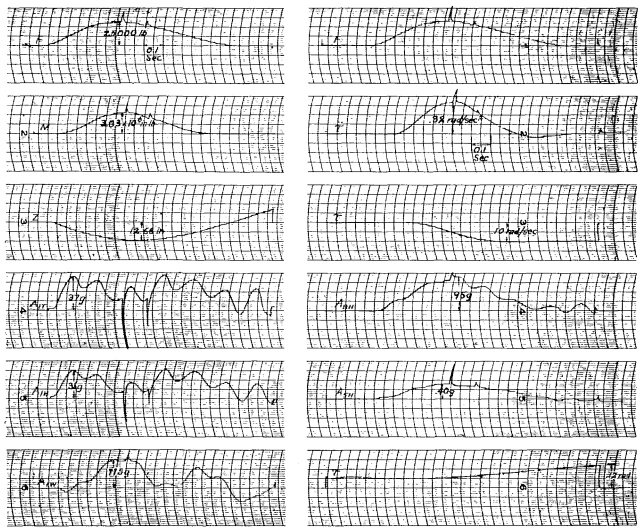

Fig. 3a. REAC solutions to impact problem—flexible case. V_x = 185 ft. per sec., τ_0 = 3°, $\dot{Z}_0$ = 4 ft. per sec.

The most difficult quantity to measure—the rate of descent—proved to be, perhaps, the most important. Attempts to use doppler radar were unreliable over anything but a glassy smooth sea. Consequently, a photo-theodolite system was installed at the landing range. The rate of descent could be obtained with reasonable accuracy from motion picture film of each landing trial.

The range of parameters investigated was limited by the structural strength of portions of the airframe and by the handling characteristics of the aircraft. The strength of the engine mount structure (limit load factor of 4.5) placed a limitation on the maximum rate of descent obtainable. Also, it was found difficult to obtain high trim angles at high rates of descent and to obtain low trim angles at low rates of descent. However, the flights were performed within these limits and all possibilities were exploited.

Solutions of the equations of motion for hydrodynamic impact have been obtained and are presented in Tables 1 and 2 and Figs. 3a to 3e. The solutions, as obtained from the analog computer, are in the form of the time variation of the quantities being studied. These data have been reduced to the form of peak values and are reported in terms of the conditions existing at the time of peak values. Oscillograms of landings are also presented, which representatively illustrate variations of hydrodynamic force and moment, motions of the aircraft, and the acceleration response of the aircraft having significance in the structural dynamics problem.

Discussion

It is a well-known result that the response of a simple mechanical system to suddenly applied forces is a func-

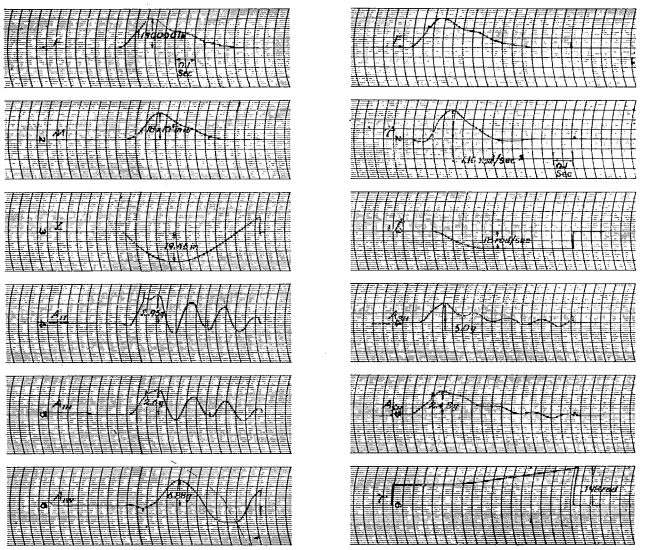

FIG. 3b. REAC solutions to impact problem—flexible case. V_x = 185 ft. per sec., τ_0 = 6°, $\dot{Z}_0$ = 12 ft. per sec.

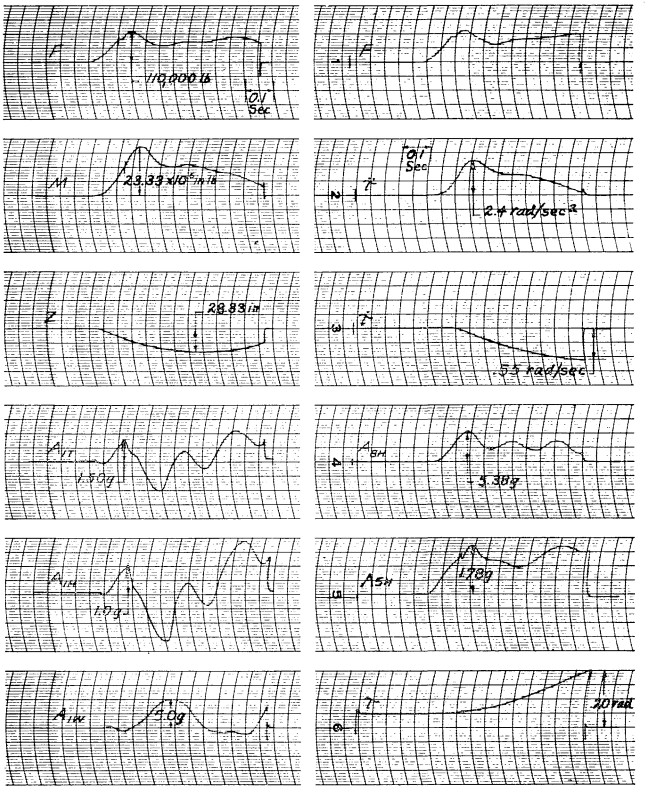

FIG. 3d. REAC solutions to impact problem—flexible case. V_x = 185 ft. per sec., τ_0 = 3°, $\dot{Z}_0$ = 12 ft. per sec.

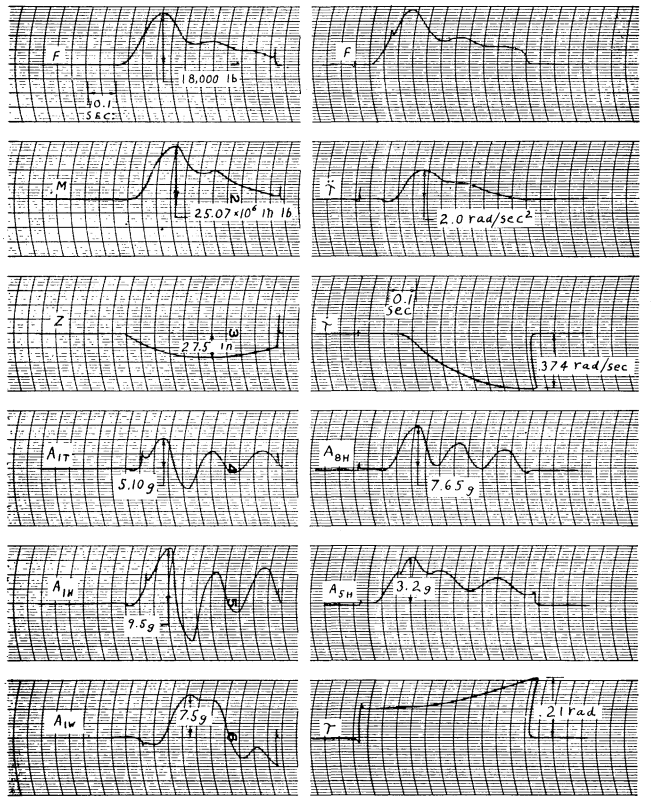

FIG. 3c. REAC solutions to impact problem—flexible case. V_x = 160 ft. per sec., τ_0 = 6°, $\dot{Z}_0$ = 12 ft. per sec.

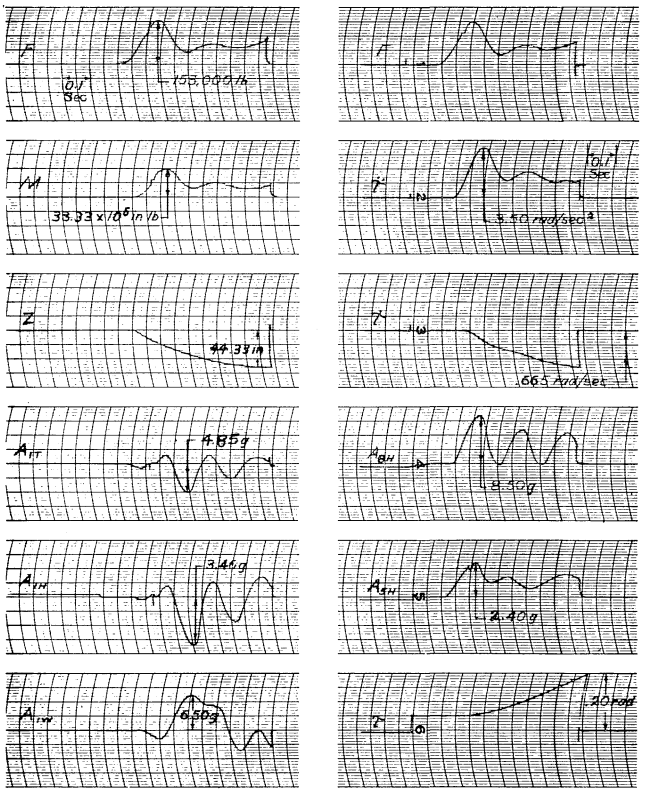

FIG. 3e. REAC solutions to impact problem—flexible case. V_x = 160 ft. per sec., τ_0 = 3°, $\dot{Z}_0$ = 16 ft. per sec.

tion of the time rate of force application and the indicial admittance of the system; thus,

$$x(t) = F_{(s)}A_{(t)} + \int_0^t (dF/dt_1)A(t - t_1)dt_1$$

The response of a mechanical system also may be expressed in terms of the response of each normal vibratory mode to the harmonics of the force. In either approach to the problem, the rate of force application or the harmonic content of the force, in conjunction with the frequency spectrum of the system, has an important bearing on the response of the system. For aircraft of high rigidity, that is, having a fundamental frequency well above $1/4t_{max}$ cycles per sec. (this is the frequency of a harmonic function which will peak at t_{max}) of the impact forcing function, the most severe distributed structural loads are generally obtained in the hardest impact condition. For the flexible aircraft having a frequency close to or within the frequency of $1/4t_{max}$, it is possible for maximum local loads to be ob-

TABLE 1
Analytical Data for the Flexible Airplane

V_x	τ_0	Z_0	F(lb)	M(in.-lb)	Z(in)	τ(rad)	$\dot{\tau}$	$\ddot{\tau}$	$A_{1H}(8)$	A_{5H}	A_{8H}	A_{1W}	A_{1T}	$Z_{at}F_{max}$	$T_{F_{max}}$	Landing No.
185	3	4	25,000	3.83×10^6	12.67	.12	.10	.32	.31	.40	.95	.775	.37	12.0	.34	1
		8	64,000	13.0×10^6	19.67	.20	.32	1.28	.875	1.2	2.75	3.15	.95	12.0	.20	2
		12	110,000	23.33×10^6	28.33	.20	.55	2.4	1.00	1.78	5.38	5.00	1.50	13.33	.125	3
	6	4	31,000	2.13×10^6	10.16	.09	.031	.06	.68	.55	.70	1.07	.76	10.0	.325	4
		8	90,000	9.33×10^6	15.33	.14	.06	.48	1.38	1.6	2.40	4.0	1.63	15.33	.225	5
		12	150,000	18.0×10^6	19.66	.198	.18	1.16	2.60	2.45	5.0	6.88	2.95	16.67	.15	6
160	3	4	23,500	3.83×10^6	13.73	.138	.115	.36	.28	.42	.90	.688	.33	13.33	.45	7
		8	60,000	12.0×10^6	21.73	.198	.346	1.24	.875	1.10	2.56	2.90	1.00	15.33	.20	8
		12	104,000	21.33×10^6	32.0	.215	.565	2.26	1.05	.170	5.20	4.50	1.00	16.67	.125	9
		16	153,000	33.33×10^6	44.33	.20	.665	3.50	3.46	2.40	8.50	6.50	4.85	16.67	.10	10
	6	4	28,500	53.33×10^6	11.33	.09	.017	.048	.575	.49	.635	.95	.65	11.00	.325	11
		8	83,000	9.13×10^6	17.07	.148	.084	.52	1.32	1.48	2.40	3.66	1.60	15.33	.20	12
		12	130,000	16.33×10^6	21.73	.21	.22	1.16	2.08	2.30	4.15	6.0	2.60	18.0	.15	13
		16	180,000	25.07×10^6	27.5	.21	.374	2.0	9.5	3.2	7.65	7.5	5.10	20.83	.125	14
	9	4	31,000	1.47×10^6	10.27	.12	.25	.11	.80	.55	.56	1.05	.85	10.0	.325	15
		8	83,000	5.93×10^6	16.27	.135	.038	.16	1.70	1.50	1.75	3.55	1.87	16.0	.225	16
		12	135,000	11.83×10^6	20.67	.173	.04	.43	2.94	2.35	3.60	6.20	3.20	17.33	.16	17
		16	185,000	18.53×10^6	26.67	.20	.14	.94	4.88	3.04	6.5	7.0	6.0	24.0	.15	18
135	3	4	23,400	4.1×10^6	14.67	.15	.133	.36	.24	.39	.85	.69	.28	14.0	.40	19
		8	55,000	11.13×10^6	25.33	.21	.36	1.12	.80	.90	2.25	2.80	.90	16.0	.20	20
		12	95,000	20.33×10^6	39.17	.20	.525	2.05	.55	1.45	4.6	4.15	.75	14.17	.125	21
		16	140,000	31.67×10^6	53.33	.21	.60	3.25	3.5	2.20	7.88	6.0	4.5	16.67	.10	22
	6	4	26,000	2.13×10^6	12.27	.105	.009	.072	.50	.45	.75	.83	.57	12.00	.35	23
		8	72,000	8.53×10^6	18.67	.17	.11	.52	1.15	1.30	2.2	3.33	1.35	17.33	.25	24
		12	120,000	16.4×10^6	23.33	.20	.25	1.12	2.30	1.96	4.15	5.25	2.90	20.00	.175	25
		16	160,000	23.67×10^6	33.33	.20	.40	1.90	3.06	2.70	6.9	6.65	4.25	23.33	.15	26
	9	4	29,200	1.60×10^6	11.87	.13	.051	.086	.65	.51	.525	.95	.69	11.8	.375	27
		8	80,000	6.13×10^6	17.60	.15	.019	.124	1.72	.130	.176	3.2	.196	16.67	.225	28
		12	120,000	11.2×10^6	23.33	.194	.075	.472	2.8	1.92	3.4	5.25	3.10	20.00	.15	29
		16	162,000	17.33×10^6	30.0	.20	.188	.96	3.8	2.64	5.75	6.5	4.70	23.33	.15	30

tained for impacts other than those having the greatest hydrodynamic force. This condition requires that a range or envelope of impact conditions be examined in order to insure that the most severe loads are utilized in the design of the aircraft structure.

Table 1 shows that a variation of t_{max} was obtained with variations in the rate of descent. The range of t_{max} was from approximately 0.10 sec. for the high rates of descent to approximately 0.40 sec. for the low rates of descent. Figs. 3a to 3e present the shape of the force and moment generated in representative landings. The spikes appearing in these curves resulted from switching equations in the REAC and may be disregarded. It may be noted that the general shape of the forces and of the moments are similar for different impact conditions with only t_{max} changing. Also, it may be seen that some delay in the generation of the moment with respect to the generation of the force was experienced. This delay is caused by the hydrodynamic center of pressure being close to the airplane center of gravity for short wetted lengths. As the wetted lengths become greater, the moment increases at a

TABLE 2
Analytical Data for the Rigid Airplane

V_x	τ_0	Z_0	F(lb)	M(in.-lb)	Z(in)	τ(rad)	$\dot{\tau}$	$\ddot{\tau}$	$A_{1H}(8)$	A_{5H}	A_{8H}	A_{1W}	A_{1T}	$Z_{at}F_{max}$	$T_{F_{max}}$	Landing No.
185	3	4	25,600	3.93×10^6	12.93	.12	.099	.32	.20	.45	.85	.45	.20	12.0	.35	31
		8	68,000	13.67×10^6	20.0	.205	.33	1.304	.74	1.225	2.74	1.25	.75	16.33	.20	32
		12	115,000	23.6×10^6	30.0	.205	.575	2.40	.52	1.97	4.75	1.97	.52	18.33	.14	33
	6	4	32,600	2.27×10^6	10.33	.09	.028	.06	.595	.58	.60	.575	.60	10.0	.30	34
		8	98,000	10.0×10^6	16.0	.14	.063	.504	1.21	1.70	.565	1.70	1.25	15.33	.20	35
		12	157,000	18.67×10^6	21.0	.18	.188	1.184	1.65	2.76	4.00	2.8	1.60	18.33	.15	36
160	3	4	23,800	4.08×10^6	14.33	.13	.115	.376	.166	.45	.87	.46	.18	13.87	.42	37
		8	61,200	12.33×10^6	22.67	.205	.34	1.20	.720	1.10	2.46	.112	.72	16.00	.20	38
		12	102,000	21.33×10^6	33.33	.195	.55	2.20	.45	1.8	4.2	1.82	.45	18.33	.15	39
		16	148,000	32.67×10^6	46.67	.20	.665	3.36	.63	2.6	6.4	2.76	.63	18.33	.10	40
	6	4	29,800	2.27×10^6	11.33	.20	.012	.048	.50	.53	.59	.55	.51	11.33	.35	41
		8	88,000	9.33×10^6	17.60	.15	.083	.524	1.03	1.54	2.18	1.52	1.05	17.00	.225	42
		12	138,000	17.07×10^6	22.67	.21	.218	1.15	1.48	2.4	3.66	2.46	1.48	18.66	.15	43
		16	190,000	25.07×10^6	29.0	.222	.36	1.9	1.90	3.36	5.50	3.36	1.90	17.66	.10	44
	9	4	33,000	1.53×10^6	10.4	.124	.061	.11	.73	.60	.495	.60	.74	10.33	.30	45
		8	91,000	6.53×10^6	16.4	.14	.033	.16	1.60	1.59	1.64	.163	1.62	16.0	.225	46
		12	143,000	12.67×10^6	21.2	.177	.046	.452	2.30	2.56	2.94	2.60	2.32	19.73	.175	47
		16	190,000	18.67×10^6	26.67	.196	.147	.912	3.00	3.44	4.35	3.48	2.96	21.67	.125	48
135	3	4	24,000	4.23×10^6	15.73	.122	.13	.384	.16	.40	.84	.45	.16	14.67	.40	49
		8	56,000	11.33×10^6	26.67	.20	.354	1.12	.675	.95	2.22	1.03	.70	16.67	.20	50
		12	92,000	19.73×10^6	41.0	.20	.52	2.0	.41	1.60	3.84	1.72	.44	18.33	.125	51
		16	138,000	30.00×10^6	56.0	.195	.60	3.06	.60	2.34	5.85	2.46	.60	16.67	.10	52
	6	4	27,400	2.33×10^6	12.67	.11	.009	.072	.425	.485	.57	.50	.425	12.33	.35	53
		8	74,000	8.67×10^6	19.07	.155	.11	.54	.85	1.35	.194	.138	.85	18.0	.225	54
		12	120,000	14.93×10^6	25.33	.195	.246	1.088	1.26	2.10	3.2	2.20	1.25	8.33	.125	55
		16	165,000	22.4×10^6	33.33	21	.40	1.76	1.66	2.96	4.75	3.04	1.74	18.33	.10	56
	9	4	30,600	1.57×10^6	11.60	.13	.05	.084	.64	.54	.475	.55	.65	11.67	.35	57
		8	80,000	6.067×10^6	18.27	.15	.018	.126	1.33	1.42	1.52	1.42	1.36	17.73	.25	58
		12	120,000	11.2×10^6	23.73	.185	.078	.496	1.90	2.20	2.60	2.26	1.90	19.33	.15	59
		16	164,000	16.67×10^6	30.00	.197	.19	.936	2.44	2.96	3.75	3.00	2.42	22.67	.125	60

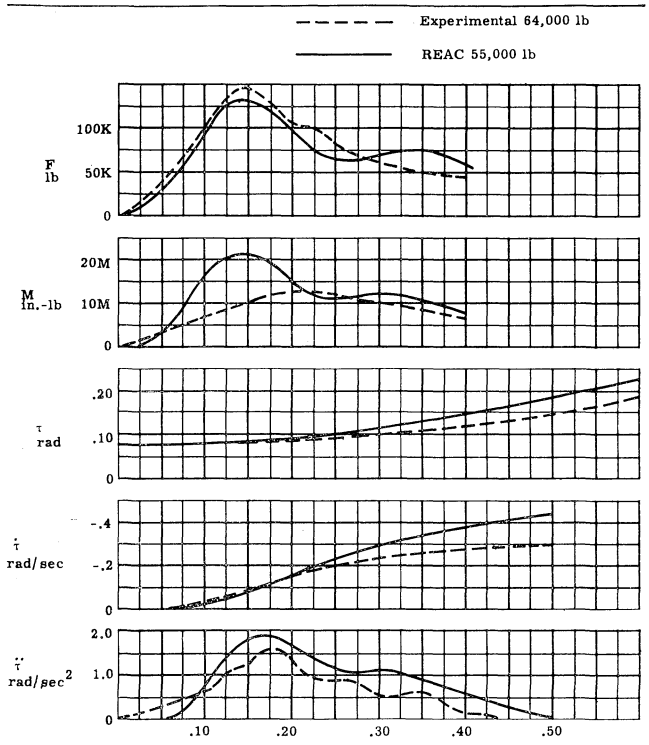

FIG. 4. Experimental vs. REAC; flight 29, landing 4.

greater rate and reaches a maximum at approximately the same instant as the force. Consequently, the loads induced by both the force and the moment must be considered in the landing analysis.

Figs. 3a to 3c show that the frequencies excited in the structure are a function of t_{max} and, hence, the rate of loading. In case 3a, the hull may be seen to respond at both 140 cycles per min. and at 390 cycles per min., the first and third modes of vibration. In case 3b it may be noted for the shorter t_{max} that the hull responds principally in the second vibratory mode at 354 cycles per min. In case 3c having t_{max} of 0.1 sec. the hull response was at 510 cycles per min. which is between the third and fourth modal frequencies.

The maximum accelerations at various locations on the airplane are given in Table 1 for each landing condition, while actual shears and moments were not obtained in this analysis. (The shear and moment distributions as a function of time could have been obtained with the equipment available, but the data obtained illustrate the point.) It may be seen that the maximum positive or negative accelerations were not necessarily obtained at the impact having the maximum force. For instance, the maximum positive bow and wing tip acceleration were obtained for landing 2, while the maximum positive stern and stabilizer tip accelerations and the maximum negative bow acceleration were obtained for landing 10. In landing 18, having the maximum force only, maximum negative accelerations were obtained at the wing tip, the stern, and the center of gravity. These results indicate that even for the rather rigid M-270 airplane an envelope of landing impacts would be necessary for accurate estimation of the landing loads.

A comparison of the maximum forces obtained for the flexible airplane analysis with the maximum forces obtained for the rigid airplane analysis affords an opportunity to study the influence of flexibility on the hydrodynamic loads. Comparing column 7 of Table 1 with column 7 of Table 2, it may be seen that in most instances the maximum forces for the flexible airplane were less than the maximum force for the rigid airplane for the same initial conditions. For the amount of flexibility present in the M-270 airplane, the maximum reduction in force was approximately 7 per cent. For more flexible airplanes, particularly if considerable weight is carried in the wings, it is conceivable that larger reductions in applied force might be obtained. This interaction between the response of the airplane and the hydrodynamic force, and the resulting reduction in applied load may have an important effect on the distributed loading experienced by the aircraft.

In regard to the influence of flexibility on the hydrodynamic moment, no definite trend is exhibited by the data. Since the moment depends among other things on the force and wetted length, there is the possibility of compensating variations in both factors for the rigid airplane case. For more flexible airplanes, appreciable changes in pitching moment may be obtained. When such information becomes available more definite conclusions may be made on the influence of flexibility on the pitching moment.

At this point, some comment on the assumptions and neglected quantities is in order. First, consider the assumption that the distributed hydrodynamic forces are given entirely in terms of the kinematics of the step. For the M-270 airplane this assumption appears

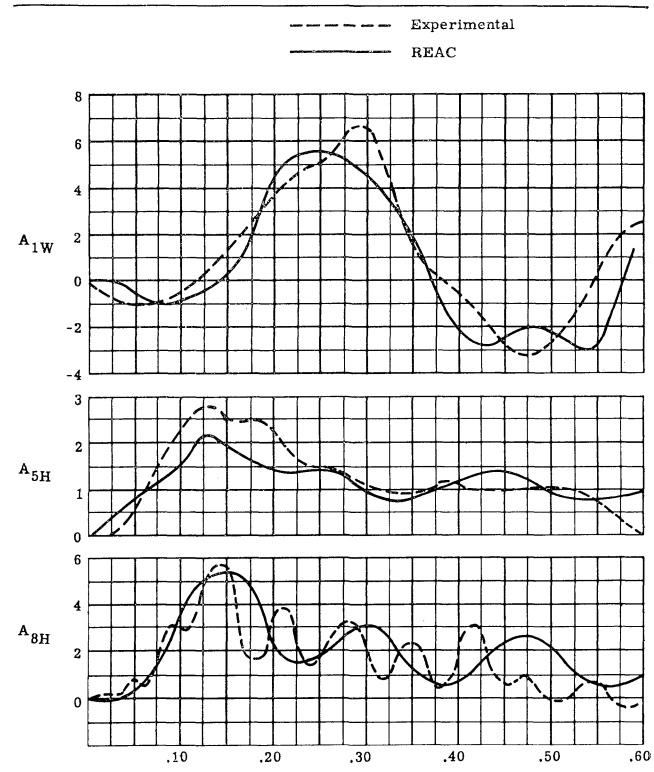

FIG. 5. Experimental vs. REAC; flight 29, landing 4.

valid, since the rigidity of the hull and vibratory modal shapes were such that adequate average values of coefficients could be used. However, for the more flexible hull, it may be necessary to describe the forces in terms of the kinematics of more than one hull station. The use of many hull stations, analogous to aerodynamic strip theory, would permit more accurate application of shape factors and of local kinematics. However, the increase in number of hull stations is accompanied by an increase in computational difficulty and for analog methods may exceed the available machine capacities.

Second, in the formulation of the hydrodynamic forces and moments two quantities have been considered as negligible. These quantities are buoyant force and moment and pitching moment due to water resistance to forward motion of the airplane. In addition, it has been assumed that the weight of the airplane is equal to the lift for the duration of impact. Some consideration of the effect of loss of lift in landing impact has been given in reference 6. The work of this reference, while treating the problem only approximately, indicates that some account for the effects of lift variation may be required. For impacts of long duration or for flexible highly coupled lifting surfaces, the lift variation might enter appreciably into the dynamics of the landing.

As landing impact becomes more critical in determining the design loads for aircraft structure (in addition to the hull bottom) and as more powerful computational methods are used, these forces may be included in the analysis.

Comparison of Experimental and Theoretical Data

Briefly reviewing, the landing impact analysis was performed for symmetric step landings in smooth water. Among the major assumptions of the analysis is that the only hydrodynamic forces acting on the airplane would be approximated by an analytical expression which is a function of the forebody shape and the kinematics of the step. Also, it was assumed that the dynamical response of the airplane is given by the rigid-body response and the superposition of the response of the first four flexible-airplane modes of vibrations. The vibratory analysis of the airplane was performed for a gross weight of 55,000 lbs. It was found after completion of the vibratory analysis that certain changes in the experimental program required the landing tests to be performed at gross weights of 64,000 lbs. and 71,000 lbs. As a consequence, some correction is to be made in interpreting the comparison of the analytical results with the experimental results. A suggested basis for this correction is in terms of the peak loads that might be expected for the rigid airplane as given in reference 6. The loads in accordance with this correction would vary as the ratio of the gross weights taken to the two-thirds power.

The experimental program was formulated for landings at discrete rates of descent, trim angle, and landing speed. However, in actual practice, it was found that only broad ranges of rate of descent and trim angle could be obtained. The analysis (REAC) is a result of discrete initial conditions; there is no direct correspondence between the analytical and nominal experimental initial conditions. One exception to this was landing 4 of flight 29, where all the initial conditions were duplicated in the REAC solution. Rate of descent ($\dot{Z}_0$) was measured relative to the earth and not the water surface, so that even 1/2 to 1-ft. waves or swells could increase or decrease effective $\dot{Z}_0$. Analytical (REAC) data are compared to experimental trends rather than individual test points for this reason.

The comparison of the time variation of the analyti-

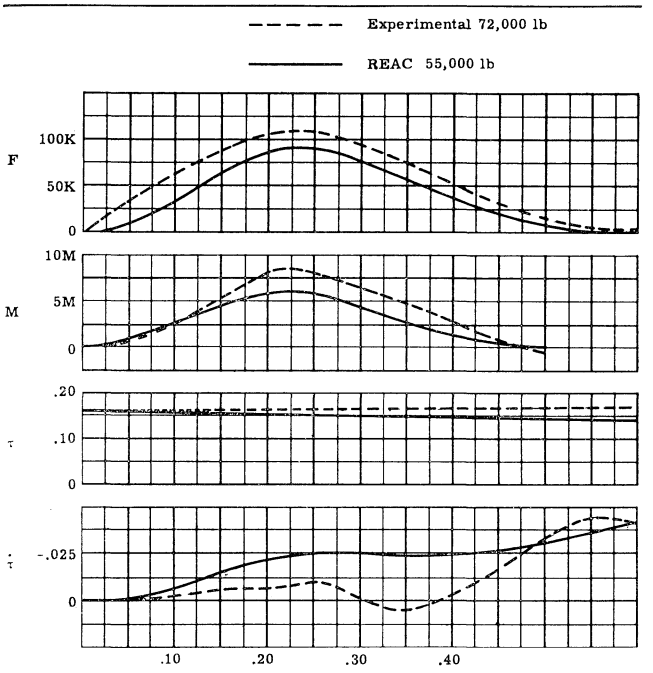

Fig. 6. Experimental vs. REAC; flight 31, landing 8.

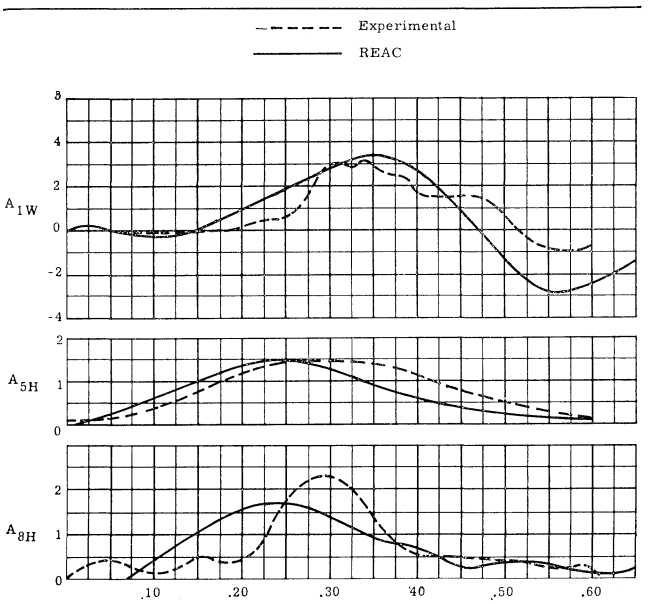

Fig. 7. Experimental vs. REAC; flight 31, landing 8.

cally determined quantities with the experimentally determined quantities for two landings may be made in Figs. 4 through 7. These Figures show the hydrodynamic force, pitching moment, trim pitching velocity, normal accelerations, and, in one instance, the pitching acceleration. In Fig. 4, the analysis was performed for the initial conditions of landing 4, flight 29. This landing represents a rather hard impact, with the variables being of sufficient magnitude that they could be determined with some precision. It is seen that the analytical results are in excellent agreement with the experimental results. The two curves are almost coincident up to t_{max} and are reasonably close after t_{max}. Excellent agreement was also obtained between analytical and experimental results for τ and $\dot{\tau}$ over the greater portion of the impact; some divergence was observed after t_{max} had occurred. In regard to the pitching moment, it may be seen that there is a considerable difference between the curves over the range of time from 0.06 sec. to 0.225 sec. No apparent reason has been found for this discrepancy. The agreement for the pitching acceleration is considered to be good in light of the manner of measurement. The shape of the analytical curve coincides reasonably with the experimental curve and the maximum values are of the same order. A comparison of the analytical acceleration response of the structure as depicted at three stations with the measured response at those stations is shown in Fig. 5. The experimental acceleration response is seen to be predicted quite well by the analytical response. The absence of the higher harmonic content in the analytical response may be attributed to using only four vibratory modes in the structural representation. As may be seen, this harmonic contribution while adding some distortion to the response does not materially affect the correlation between experiment and analysis.

Landing 8 of flight 31 for a gross weight of 72,000 lbs. also offers an opportunity to compare analytical and experimental results. Referring to Fig. 6, again it may be seen that the shape of the experimental curves for both the force and moment is given by the analytical curves. Applying the previously suggested correction for gross weight, the comparable magnitude for the experimental force for the 72,000-lb. airplane corrected to 55,000 lbs. is given by 84 per cent of the magnitude. This reduction brings the experimental force magnitude into excellent agreement with the analytical force magnitude, particularly at the maximum values. The application of the correction to the moments also tends to bring the moment magnitudes into agreement with the analytical moment magnitude. The τ variation for the analytical impact is in agreement also with that of the experiment. Comparison of the pitching velocities showed little or no agreement, and no comparison of pitching accelerations was attempted.

The structural acceleration response for the 72,000-lb. airplane may be seen in Fig. 7. Recalling that the difference in gross weights of the airplane is achieved by the addition of concentrated weights in the hull about the airplane center of gravity, it is to be expected that the vibratory characteristics of the hull would be greatly influenced, and the wing to a lesser degree, by the presence of these weights. Comparing the experimental acceleration response of the 72,000-lb. airplane with the calculated response for the 55,000-lb. airplane, it may be seen that this occurs. The shape and magnitude of the calculated center of gravity and wing tip accelerations are in reasonable agreement with the experimental accelerations. The experimental bow accelerations, apparently showing the influence of the added hull weight, are seen to behave somewhat differently from the calculated accelerations. In light of the above discussion, it is felt that where some basis for comparison with the heavy airplane existed, the analytical results are in agreement with the experimental results.

Figs. 3a to 3d present the maximum values of force and of structural acceleration from the analysis as a function of rate of descent for the different initial trim angles and forward speeds. For purposes of comparison, experimental values having approximately the same initial trim angles and forward speeds are also shown against rate of descent. The analytical results for the structural response of the structure are in good agreement with the experimental data. Reduction of experimental data for the hydrodynamic force was not done for all landings. However, at a forward speed of 160 ft. per sec., the agreement between the analytically predicted force and the experimentally determined force is good in trend and magnitude.

The above comparisons of experimental data with analytical data have shown that the analytically determined results have described accurately the landing impact conditions. The correlation of hydrodynamic forces and moments has indicated that the representation of these forces and moments in the equations of motion has been substantiated. The structural response as given by the equation of motion agrees very well with the actual structural response of the airplane, and indicates that the flexibility of the airplane was adequately represented by the flexible modes of the analysis. The response of the rigid airplane in pitch given in the analysis was in agreement with the experimental observed response. In light of this, it is believed that the hydrodynamic step impact and the dynamic response for the flexible seaplane may be accurately given by the method of analysis presented in this paper.

Conclusions and Recommendations

A theoretical method of computing the dynamical impact landing, including the effects of structural flexibility and continuous trim variation, has been developed in "closed" form. This method, utilizing an electronic analog computer, permits rapid study of a wide range of initial conditions for the impact problem.

The dynamic acceleration response of the M-270

(*Continued on page 216*)

diameter and thickness of the specimens to obtain a measure of the accuracy of the theory.

Twenty-one test specimens with lengths varying from 4.0 to 89.0 inches were utilized in the tests. The material, 2024-T3 aluminum alloy, and a D/t ratio of 70.5 were used throughout the experiment.

For convenience, two relations from reference 1 are shown below:

$$(D/t)_{\text{optimum}} = 2[k_2^2 E/\pi(P/L^2)]^{1/3} \quad (1)$$

$$P/L^2 = 8f^3_{\text{optimum}}/k_2\pi E_t^{3/2}E^{1/2} \quad (2)$$

Eq. (1) gives the optimum cross section for a given material and structural index. Eq. (2) was used to plot the optimum stress versus structural index curve shown in Fig. 1. Note that to plot this curve, it is only necessary to have the material properties. These were obtained from compression tests on the column material.

After data on the buckling or crippling load had been obtained for each column, it was possible to plot the test data as shown in Fig. 1. As the length was varied, the test points approached the optimum curve and then broke away again. The optimum point was obtained as $(P/L^2)^{1/2} = 6.9$.

Substituting the experimentally obtained optimum structural index into Eq. (1), an optimum D/t ratio of 74.2 was obtained. An error of 5.25 per cent resulted when this value was compared with the actual D/t ratio of the specimens. A value of 0.84 was used for k_2 in Eqs. (1) and (2), on the basis of experimental data previously obtained at the University of California at Los Angeles, Calif.[2]

References

[1] Shanley, F. R., *Principles of Structural Design for Minimum Weight*, Journal of the Aeronautical Sciences, Vol. 16, No. 3, pp. 133–149, March, 1949.

[2] Needham, R. A., *Compression Tests of Round Tubes*, Memorandum Report to F. R. Shanley, Univ. of California, College of Engineering, Los Angeles, Calif., July 18, 1954.

On Optimum Nose Shapes for Missiles in the Superaerodynamic Region

David H. Dennis

Aeronautical Research Scientist, Ames Aeronautical Laboratory, NACA, Moffett Field, Calif.

November 27, 1957

W. J. CARTER[1] and I. D. Chang[2] have calculated the shape of the body of revolution of given length and base diameter, having minimum drag in hypervelocity free-molecule flow, assuming specular reflection from a smooth surface. With this assumption, the expression defining surface pressure coefficient is the same as that for Newtonian flow except for a constant factor of 2. Accordingly, the minimum drag body should have the same shape, including a small flat nose, as that derived by Newton.[3] The parametric equations defining this shape are

$$y = (y_1/4)\,[(1 + y'^2)^2/y'^3]$$

$$x = (y_1/4)\,[(3/4y') + (1/y'^2) - (7/4) + \ln y']$$

where y_1 is the nose radius.[4]

The flat nose results from the restriction on body length. If the length is not fixed, the minimum drag shapes have sharp noses. For example, the cone is the minimum drag shape of given surface area and base diameter.[4]

As a final point it may be noted that since the local drag on a body in the flows considered here depends only on local slopes and body radii, the first integral to the Euler equation may be written immediately and the body coordinates in terms of body slopes are easily deduced.

References

[1] Carter, W. J., *Optimum Nose Shapes for Missiles in the Superaerodynamic Region*, Journal of the Aeronautical Sciences, Vol. 24, No. 7, pp. 527–532, July, 1957.

[2] Chang, I. D., *On Optimum Nose Shapes for Missiles in the Superaerodynamic Region*, Journal of the Aeronautical Sciences, Readers' Forum, Vol. 25, No. 1, pp. 57, 58, January, 1958.

[3] Newton, Isaac, *Principia-Motte's Translation Revised*, pp. 333, 657–661; Univ. of California Press, Berkeley, 1946.

[4] Eggers, A. J., Jr., Resnikoff, Meyer M., and Dennis, David H., *Bodies of Revolution Having Minimum Drag at High Supersonic Airspeeds*, NACA Report 1306, 1957 (Supersedes NACA TN 3666).

Structural and Impact Loads for the Flexible Airplane . . .

(*Continued from page 170*)

airplane was obtained from experimental measurements over a range of impact conditions. From these measurements the hydrodynamic force and moment on the airplane were obtained. The most critical parameter in measuring the effects of landing impact was found to be the rate of vertical descent.

A comparison of the experimental impact data with the results of the analysis showed that the analytical results generally were in good agreement with the experimental results. This agreement includes both time variation and magnitude. It is concluded that the hydrodynamic step impact and the dynamic response of the flexible seaplane may be accurately given by the method of analysis presented in this paper.

The response of the flexible airplane was found to be a function of both the magnitude and shape of the forcing function. The maximum inertial loading for some structures was not obtained for the conditions of maximum hydrodynamic loading. In order to obtain the maximum loads for the flexible airplane it was necessary to study a range of landing impacts.

The inclusion of airplane flexibility in the equations of motion tended to reduce the hydrodynamic force obtained for the rigid airplane. In this instance the maximum reduction was of the order of 7 per cent. However, for a more flexible airplane this reduction may be of a large magnitude.

References

[1] Schwab, R. H., and Widmayer, E., Jr., *Martin Model 270 Water Loads Investigation—Structural and Impact Loads Considering Airplane Flexibility*, Martin ER 7515, November, 1955.

[2] King, Douglas A., and Adams, Richard C., *Martin Model 270 Water Loads Investigation: Hull Bottom Pressures and Impact Loads*, Martin ER 7516, July, 1955.

[3] Biot, M. A., and Bisplinghoff, R. L., *Dynamic Loads on Airplane Structures During Landing*, NACA ARR 4H10 (WR-W-92), October, 1944.

[4] Mayo, W. L., *Hydrodynamic Impact of a System with a Single Elastic Mode—I Theory and Generalized Solution with an Application to an Elastic Airframe*, NACA Report 1074, 1952.

[5] Milwitzky, Benjamin, *Generalized Theory for Seaplane Impact*, NACA Report 1103, 1952.

[6] Benscoter, Stanley V., *Effect of Partial Wing Lift in Seaplane Landing Impact*, NACA TN 1563, 1948.